

Multisite Analyses of Spectral-Biophysical Data for Wheat

C. L. Wiegand and S. J. Maas

USDA/ARS, Subtropical Agricultural Research Laboratory, Remote Sensing Research Unit, Weslaco, Texas

J. K. Aase

USDA/ARS, Northern Plains Soil and Water Research Laboratory, Sidney, Montana

*J. L. Hatfield**

USDA/ARS, Cropping Systems Research Laboratory, Lubbock, Texas

P. J. Pinter, Jr. and R. D. Jackson

USDA/ARS, U. S. Water Conservation Laboratory, Phoenix, Arizona

E. T. Kanemasu[†] and R. L. Lapitan[‡]

Agronomy Department, Kansas State University, Manhattan

Reflectance factors and biophysical plant measurements for wheat (*Triticum aestivum* L.) experiments conducted at Lubbock, Texas, Manhattan, Kansas, Phoenix, Arizona, Sidney, Montana, and Weslaco, Texas were fit by various equation forms for six currently used vegetation indices (VI): *n*-space greenness (GVI), perpendicular (PVI), NIR/RED ratio (RVI), soil adjusted (SAVI2), normalized difference (NDVI), and transformed soil

adjusted (TSAVI). The objective was to produce relations from the data pooled across all locations that could be recommended for general use for wheat. Data were analyzed by premaximum leaf area (pre- L_{max}), post-maximum leaf area (post- L_{max}), and whole season portions of the growing season. Leaf area index (L) was best estimated from RVI and TSAVI by linear equations, from NDVI and TSAVI by exponential equations, and from the orthogonal indices GVI and PVI equally well by power and quadratic equation forms. These equation forms gave coefficients of determination (R^2) that ranged from 0.72 to 0.86, and root mean square errors (RMSE) in estimating L that ranged from 0.63 to 0.90 across locations and measurements that differed in soils, sun angles, cultivars, agronomic treatments, and radiometers. The single best equation form for estimating L from VI across

* Present address: National Soil Tilth Laboratory, Ames, Iowa.

† Present address: Department of Agronomy, University of Georgia, Griffin.

‡ Present address: Natural Resource Ecology Laboratory, Colorado State University, Fort Collins.

Address correspondence to Craig L. Wiegand, USDA/ARS, Remote Sensing Unit, 2413 E. Highway 83, Weslaco, TX 78596.

Received 16 September 1991; revised 14 March 1992.

all VI was the power form. The orthogonal indices GVI and PVI were more responsive to canopy architecture than the ratio vegetation indices, and GVI ranked as the best single index. Equations for estimating fractional absorbed photosynthetically active radiation (FPAR) from VI given herein agree well with empirical and semitheoretical equations and their coefficients found in the literature. Our results demonstrate the robustness of vegetation indices across experiment variables and measurement conditions, and provide general functional relations that should be useful for wheat.

INTRODUCTION

Hydrologists, ecologists, plant growth and yield modelers, agricultural meteorologists, water and soil conservationists, plant breeders, and other prospective users of spectral-biophysical relationships need generally applicable equations. Such equations can result from the pooling of data from geographically separated locations where careful plant and spectral measurements have been taken, and procedures are well documented. Such equations are generally lacking for major crops for a variety of reasons, including the proprietary nature of the data and the interlocation variation due to differences in sun zenith angle (latitude, planting data, and time of day of observations), soil and surface conditions, instruments and measurement techniques, canopy architecture (leaf angle, canopy openness, and height), and cultural practices (row spacing, plant population, and fertilization) (Wiegand et al., 1990). Radiative transfer models such as SAIL (Verhoef, 1984; Goel, 1988) have become popular for explaining systematically controlled variation such as sun and look angles in diurnal studies, but they are less able to summarize seasonal data where soil background reflectance has fluctuated due to changing surface moisture conditions and cultivation, and canopy architecture has changed with crop development.

To help provide the needed relationships, the Spectral-Agronomic Multisite-Multicrop Analyses (SAMMA) Project (Wiegand and Hatfield, 1988) was initiated. Under SAMMA, reflectance data from handheld and boom-mounted multi-band radiometers and agronomic or biophysical plant measurements have been pooled across lo-

cations for uniform analyses of corn (*Zea mays* L.), wheat (*Triticum aestivum* L.), grain sorghum (*Sorghum bicolor* Moench), soybean (*Glycine max* Merr.), and cotton (*Gossypium hirsutum* L.). In this paper, the spectral reflectance and biophysical data for wheat experiments conducted at Lubbock, Texas, Manhattan, Kansas, Phoenix, Arizona, Sidney, Montana, and Weslaco, Texas were analyzed using the same equation forms. The objectives were to determine statistically appropriate empirical relations within and among locations and to generalize the relations among leaf area index, light absorption, and canopy reflectance.

METHODS AND MATERIALS

Data from five locations (Table 1) were pooled from experiments documented as follows: Lubbock and Manhattan '85 (Reginato et al., 1988; Major et al., 1988; Garcia et al., 1988); Manhattan '83 (Lapitan, 1986; Wall and Kanemasu, 1990); Phoenix (Pinter et al., 1985; Jackson and Pinter, 1986; Maas et al., 1989); Sidney (Aase and Tanaka, 1984); Weslaco (Wiegand and Richardson, 1987; 1990). At least 15 additional studies had been identified as data sources (Wiegand and Hatfield, 1988), but changes in and redirection of personnel, computer system and software changes, and lack of funds to finance the reconstruction and formatting of data sets made them inaccessible. Observations more frequent than approximately weekly were deleted in all data sets, and when diurnal measurements were reported, midday observations were used when available.

Field experiments and biophysical measurements. The latitude and longitude of each test site, the year of crop harvest, the main treatments used, cultivars, row spacing, height from which observations were made, dates of cardinal phenologic events, maximum leaf area index (L_{max}) achieved, soil type, and fertilization are summarized in Table 1.

Green leaf area index (L , m^2/m^2) was determined by harvesting a known row length or selecting median sized plants from a sample of plants, excising their leaves, passing them through an area meter, and expanding the area of leaves to that per m^2 of ground area occupied by the sample, except at Sidney and Weslaco. At those two

Table 1. Treatment, Cultivars, Soils, Height above Ground of Observations, and Growth and Development Characteristics of Wheat in the Experiments of this Study

Location; Lat., Long. (deg)	Year	Treatments Used	Cultivars	Phenology (DOY)				Fertilizer (kg/ha)	Row Spacing (m)	Height of Obs. (m)	Soil Type		
				L_{max}^a	Emergence	Anthesis	Physiol. Maturity						
Lubbock, TX; 36.52°N 109.05°W	1985	Rainfed, ample irrig., lo N, med. hi N	Colt	1.9	340	~ 105	~ 150	N-60 N-160	0.20	1.2 or 2.8	Olton clay loam		
			TAM 101	2.0									
				1.5									
				1.8									
Manhattan, KS; 39.15°N 96.62°W	1985	Rainfed, ample irrig., lo N, med. hi N	Colt	1.8	~ 300	129	147	N-60 N-160	?	1.2 or 2.8	Muir silt loam		
			Newton	6.4									
				1.8									
				4.9									
Phoenix ^a AZ; 33.43°N 112.02°W	1983	No stress (NS), early stress (ES)	Ciano 79	6.6	13	104	143	N-258 P-18	0.18	1.8	Avondale loam		
			Genaro 81	6.7								108	143
			Seri 82									104	143
			Yecora 70									103	139
Sidney, MT; 47.77°N 104.25°W	1982	Fallowed WW, ^c standing stubble WW, fallowed SW ^c	Norstar	3.1	~ 268	183	211	N-45 P-0 K-0	0.34 (WW) 0.23 (WW)	1.8	Williams loam		
			Norstar	2.2									
			Len	2.1	~ 132	191	222						
Weslaco, TX; 26.16°N 97.96°W	1984	2 fertil., 2 row directions	Aim	3.8	326	59	94	N,P,K-0 N-100 P-33 K-33	0.20	1.2	Raymond- ville clay loam		
			Nadadores	4.0								88	116
Manhattan, KS; 39.15°N 96.62°W	1983	2 row spacings, 2 row directions	Newton	5.3	~ 295	146	169	N-109	0.18 0.36	7.6	Muir silt loam		
				4.2									

^a Maximum achieved in any replicate of the treatment regardless of cultivar.

^b Phenology observations are for no-stress treatment by cultivars; yield are for no-stress and early stress treatments by cultivar.

^c WW = winter wheat; SW = spring wheat.

sites, L was estimated through Feekes growth stage 5, leaf sheaths strongly erect (Large, 1954), from above-ground dry matter (DM, g/m²) from the equation (Aase, 1978)

$$L = 0.0026 + 0.0114(\text{DM}) \quad (1)$$

and after growth stage 5 from dry green leaf mass (LM, g/m²) using the equation (Aase, 1978), as verified at Weslaco (LeMaster et al., 1980),

$$L = -0.0028 + 0.0202(\text{LM}) \quad (2)$$

The L data for all sites were smoothed using either exponential polynomials of time (Hughes and Freeman, 1967; Wiegand et al., 1989) machine procedures, or manual graphical methods.

Above-ground dry phytomass (DM, g/m²) was provided by the same plant samples that provided L for all sites except Sidney. The fraction of photosynthetically active radiation absorbed (FPAR) was provided only for Manhattan '83 and Weslaco.

Soil lines and vegetation indices. Bidirectional reflectance factor measurements (Richardson, 1981;

Jackson et al., 1987; Walter-Shea and Biehl, 1990) were acquired with an Exotech 100-BX¹ multi-band radiometer at Lubbock and Manhattan in 1985 and with a Barnes modular-multiband radiometer (MMR; Robinson et al., 1979) at Phoenix using wavelengths (Table 2) similar to those of the Thematic Mapper on Landsat. Measurements at Sidney and at Manhattan in 1983 were made with an Exotech 100A (EXO) whose bands are similar to those of the multispectral scanner on Landsat. Measurements at Weslaco were made with the two-band Mark II radiometer (Tucker et al., 1981) whose bands are the same as the RED and NIR bands of the Exotech 100-BX and Barnes MMR used at Lubbock, Manhattan, and Phoenix (Table 2). The EXO and MMR instruments had 15° fields of view (FOV) whereas the FOV of

¹ Mention of trade names does not infer preferential treatment nor endorsement by the USDA over similar products available from other sources.

Table 2. Instruments, Wavelengths, and Their Use by Experimental Sites

Lubbock, Manhattan '85 EXOTECH 100-BX, Phoenix BARNES MMR 12-1000		Sidney, Manhattan '83 EXOTECH 100A		Weslaco MARK-II		Designation, Color
Band	μm	Band	μm	Band	μm	
1	0.45-0.52					Blue
2	0.52-0.60	1	0.50-0.60			Green
3	0.63-0.69	2	0.60-0.70	1	0.63-0.69	Red
		3	0.70-0.80			Near-IR
4	0.76-0.90	4	0.80-1.10	2	0.76-0.90	Near-IR

the Mark II was 24°. Measurements were made looking vertically downward from the handheld and boom-mounted heights given in Table 1.

The soil line defined by

$$\text{NIR} = a(\text{RED}) + b, \quad (3)$$

where NIR and RED are reflectance factors in the near-infrared and visible red bands, respectively, b is the intercept, and a is the slope was determined (Fig. 1) for each site and instrument

(Table 2). The bands designated NIR and RED for the multiband radiometers of this study are specified in Table 2. In Figure 1, the data used for light (or dry) soil defines the upper end and those used for dark (or wet) soil define the lower end of the soil line. The bare soil data for Lubbock and Phoenix were provided for the same soil and instrument, but from other experiments, by D. F. Wanjura (personal communication, Jan. 1991) and by P. J. Pinter, Jr. (personal communication, Oct. 1990), respectively. Manhattan is the only

Table 3. Vegetation Index Equations by Location

Location	Radiometer	Vegetation Index Equations	Eq. No.
Lubbock	EXO 100BX	$\text{GVI} = -0.276(\text{MMR2}) - 0.678(\text{MMR3}) + 0.681(\text{MMR4}) - 1.44$	(Ga)
		$\text{PVI} = -0.783(\text{MMR3}) + 0.622(\text{MMR4}) - 1.34$	(4a)
		$\text{SAVI2} = \text{MMR4} / (\text{MMR3} + 2.30)$	(6a)
		$\text{TSVI} = (1.208(\text{MMR4}) - 1.459(\text{MMR3}) - 3.36) / (\text{MMR3} + 1.208\text{NIR} - 3.36)$	(8a)
Manhattan, '85	EXO 100BX	$\text{GVI} = -0.359(\text{MMR2}) + 0.618(\text{MMR3}) + 0.699(\text{MMR4}) - 1.30$	(Gb)
		$\text{PVI} = -0.787(\text{MMR3}) + 0.617(\text{MMR4}) - 1.25$	(4b)
		$\text{SAVI2} = \text{MMR4} / (\text{MMR3} + 1.58)$	(6b)
		$\text{TSVI} = (1.276(\text{MMR4}) - 1.628(\text{MMR3}) - 2.58) / (\text{MMR3} + 1.276(\text{MMR4}) - 2.58)$	(8b)
Phoenix	MMR	$\text{GVI} = -0.333(\text{MMR2}) - 0.552(\text{MMR3}) + 0.764(\text{MMR4}) - 2.35$	(Gc)
		$\text{PVI} = -0.729(\text{MMR3}) + 0.684(\text{MMR4}) - 1.74$	(4c)
		$\text{SAVI2} = \text{MMR4} / (\text{MMR3} + 2.42)$	(6c)
		$\text{TSVI} = (1.064(\text{MMR4}) - 1.132(\text{MMR3}) - 2.74) / (\text{MMR3} + 1.064(\text{MMR4}) - 2.74)$	(8c)
Sidney	EXO 100A	$\text{GVI} = -0.452(\text{EXO1}) - 0.676(\text{EXO2}) + 0.231(\text{EXO3}) + 0.534(\text{EXO4}) - 0.72$	(Gd)
		$\text{PVI} = -0.813(\text{EXO2}) + 0.582(\text{EXO4}) - 0.894$	(4d)
		$\text{SAVI2} = \text{EXO4} / (\text{EXO2} + 1.107)$	(6d)
		$\text{TSVI} = (1.40(\text{EXO4}) - 1.96(\text{EXO2}) - 2.17) / (\text{EXO2} - 1.40(\text{EXO4}) - 2.17)$	(8d)
Weslaco	MK-II	$\text{PVI} = -0.815(\text{MK1}) + 0.580(\text{MK2}) - 0.41$	(4e)
		$\text{SAVI2} = \text{MK2} / (\text{MK1} + 1.92)$	(6e)
		$\text{TSVI} = (1.267(\text{MK2}) - 1.605(\text{MK1}) - 3.08) / (\text{MK1} - 1.267(\text{MK2}) - 3.08)$	(8e)
Manhattan '83	EXO 100A	$\text{GVI} = -0.506(\text{EXO1}) - 0.633(\text{EXO2}) + 0.198(\text{EXO3}) + 0.551(\text{EXO4}) + 0.24$	(Gf)
		$\text{PVI} = -0.822(\text{EXO2}) + 0.570(\text{EXO4}) - 0.32$	(5f)
		$\text{SAVI2} = \text{EXO4} / (\text{EXO2} + 0.35)$	(6f)
		$\text{TSVI} = (1.443(\text{EXO4}) - 2.082(\text{EXO2}) - 0.74) / (\text{EXO2} - 1.443(\text{EXO4}) - 0.74)$	(8f)
All	Any	$\text{RVI} = \text{NIR}/\text{RED}$ where NIR = MMR4, EXO4, MK2; RED = MMR3, EXO2, MK1	(5)
		$\text{NDVI} = (\text{NIR} - \text{RED}) / (\text{NIR} + \text{RED})$	(7)

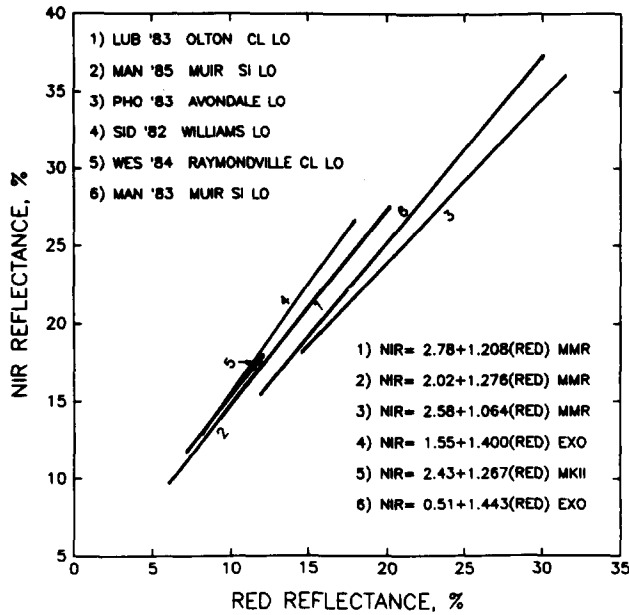


Figure 1. Comparison of soil lines by location and radiometer.

location at which data were taken with two different instruments over the same soil.

Six extensively used or recently recommended vegetation indices were calculated, four of which are referenced to the soil and should minimize soil variation among sites (Wiegand and Hatfield, 1988). The four- and three-band greenness vegetation indices (GVI) of Table 3 were calculated by the n -space procedure of Jackson (1983) with the modification that the greenness of the soil plane was added algebraically to the greenness equation. This modification makes the 2-space greenness identical to the perpendicular vegetation index (PVI) (Richardson and Wiegand, 1977) defined by the perpendicular to a line,

$$PVI = (NIR - a \text{ RED} - b) / (1 + a^2)^{1/2}, \quad (4)$$

where a and b are as defined in Eq. (3). As shown by the equations in Table 3, the traditional 4-space GVI (GVI4) was calculated for the Exotech 100-A whose bands are similar to those of the Landsat MSS, while a 3-space GVI (GVI3) was calculated from Bands 2, 3, and 4 of the MMR because we found for corn (Wiegand et al., 1990) that GVI3 and GVI4, using Bands 1, 2, 3, and 4, were almost identical for the MMR.

Two other vegetation indices calculated and used were the ratio vegetation index (RVI) (Pearson and Miller, 1972).

$$RVI = NIR / RED, \quad (5)$$

and a modification of it, the soil adjusted vegetation index (SAVI2) (Major et al., 1990),

$$SAVI2 = (NIR) / (RED + b/a). \quad (6)$$

The extensively used normalized difference vegetation index (NDVI) (Rouse et al., 1974),

$$NDVI = (NIR - RED) / (NIR + RED), \quad (7)$$

and its modification to consider soil background, the transformed soil adjusted vegetation index (TSAVI) (Baret et al., 1989),

$$TSAVI$$

$$= a(NIR - aRED - b) / (RED + aNIR - ab), \quad (8)$$

were also calculated.

Data pairing. Leaf area index measurements made at about weekly intervals were summarized to treatment means and paired with treatment means of spectral measurements. When observation dates differed, L was interpolated to the date of the spectral measurements using the polynomial smoothing equations or manually smoothed graphs. The data were divided into pre- L_{max} , post- L_{max} , and full growing season portions for particular analyses to deal with nonliving phytomass effects on observations (Wiegand and Hatfield, 1988). Data for the last date in the pre- L_{max} portion were included as the first date in post- L_{max} sets when analyzed separately, but data for the tie point were not repeated in the full season data sets.

Analysis procedures. Data were first analyzed within location by instrument and year to determine whether cultivars or agronomic management affected equation coefficients. SAS (SAS Institute, 1988) nonlinear procedures and the model form

$$Y = C_i \{1 - A_i \exp[-B_i(X)]\} \quad (9)$$

were used, where

Y = fractional PAR absorption (FPAR) or any of the six vegetation indices GVI, PVI, RVI, SAVI2, NDVI, or TSAVI,

X = green leaf area index L ,

C_i = the asymptotically limiting value of Y at large L ,

A_i = the value of $(1 - Y)$ at $L = 0$ for variables normalized to 1.0 (FPAR, NDVI) (Wiegand

and Hatfield, 1988), but a fitting coefficient for variables not normalized to 1.0,

B_i = an absorption-scattering coefficient for the wavebands used that is leaf angle distribution and solar zenith angle dependent,
 i = a treatment identifier.

The three-parameter model of Eq. (9) was used because it describes the dependence of VI, FPAR, crop yield, and the reciprocal of canopy resistance to water vapor transfer ($1/r_c$) on leaf area index (Wiegand and Richardson, 1984; Sellers, 1985, 1987; Choudhury, 1987; Wiegand and Hatfield, 1988). All increase rapidly as L increases to about 3, and then approach limiting values as L increases further.

The following hypotheses were tested:

1. FM vs. RM1 = $C_i A_i B_i$ vs. $C A_i B_i$; if significant, the C 's differ in Eq. (9).
2. RM1 vs. RM2 = $C A_i B_i$ vs. $C A B_i$; if significant, the A 's differ in Eq. (9).
3. RM2 vs. RM3 = $C A B_i$ vs. $C A B$; if significant, the B 's differ in Eq. (9). In hypotheses 1, 2, and 3, above, the full model (FM) symbolized by $C_i A_i B_i$ means C , A , and B are each unique for each treatment; the model reduced by one parameter (RM1) symbolized by $C A_i B_i$ means the C is common among treatments, but A and B are unique for each treatment; the model reduced by two parameters (RM2) symbolized by $C A B_i$ means C and A are common for all treatments but B is unique for each. If none of the tests is significant, the fully reduced model (RM3) applies; that is, all treatments can be represented by a common set of C , A , and B coefficients.

Significance of hypotheses was determined by an asymptotic F-test (C. Perry, USDA, Statistical Reporting Service, Fairfax, VA, June, 1984, personal communication; Milliken and DeBruin, 1978):

$$F_{(H_i)} = \frac{N - \text{PFM}}{\text{PFM} - \text{PRM}} \times \frac{\text{RSS}(\text{model reduced by } H_i) - \text{RSS}(\text{Full model})}{\text{RSS}(\text{full model})},$$

where

N = the number of observations,

RSS = residual sum of squares,

PFM = the number of parameters in the full model of the hypothesis tested (the one on the left in each hypothesis statement above),

PRM = the number of parameters in the reduced model (the one to the right of "vs." in each hypothesis statement).

For example, for three treatments, PFM = 9, PRM1 = 7, PRM2 = 5, and PRM3 = 3.

The growing seasons differed with latitude, and spectral observations were made at differing local standard times of day among locations [1140–1200 h at Lubbock; mostly 1100–1300 h at Manhattan; centered on 1035 h at Phoenix (Jackson and Pinter, 1986), 0830–0840 h at Sidney (Aase and Tanaka, 1984), and 1300–1400 h at Weslaco] as documented in the data sets or the cited references. The coordinates of each site (Table 1), the dates, and the time of day of the observations were used to calculate the solar zenith angles (Z) at the time of the observations from ephemeris equations.

Because biophysical parameter estimates from all observation systems in use are needed, we also used linear, quadratic, power, and two-parameter exponential equations in which VI was the independent variable and the plant biophysical parameters and FPAR were the dependent variables. These equations were determined for data pooled across locations for pre- L_{\max} , post- L_{\max} , and full season data sets.

RESULTS

Figure 2, in which L , DM, RED, and NIR reflectance are presented versus day of year (DOY) by contrasting treatments (Table 1) for each of the five locations shows how the growing season varied with latitude and elevation. It coincided closely only for Lubbock and Manhattan. Mean leaf area index (L) did not exceed 2 at Lubbock, 3 at Sidney, and 4 at Weslaco but approached 5 at Manhattan and 6 at Phoenix. (Leaf area index maxima, L_{\max} , are lower in Fig. 2 than in Table 1, where the values given are the maxima achieved in any replicate of the treatment while those in Fig. 2 are means for all replicates within the selected treatment.) The only locations with simi-

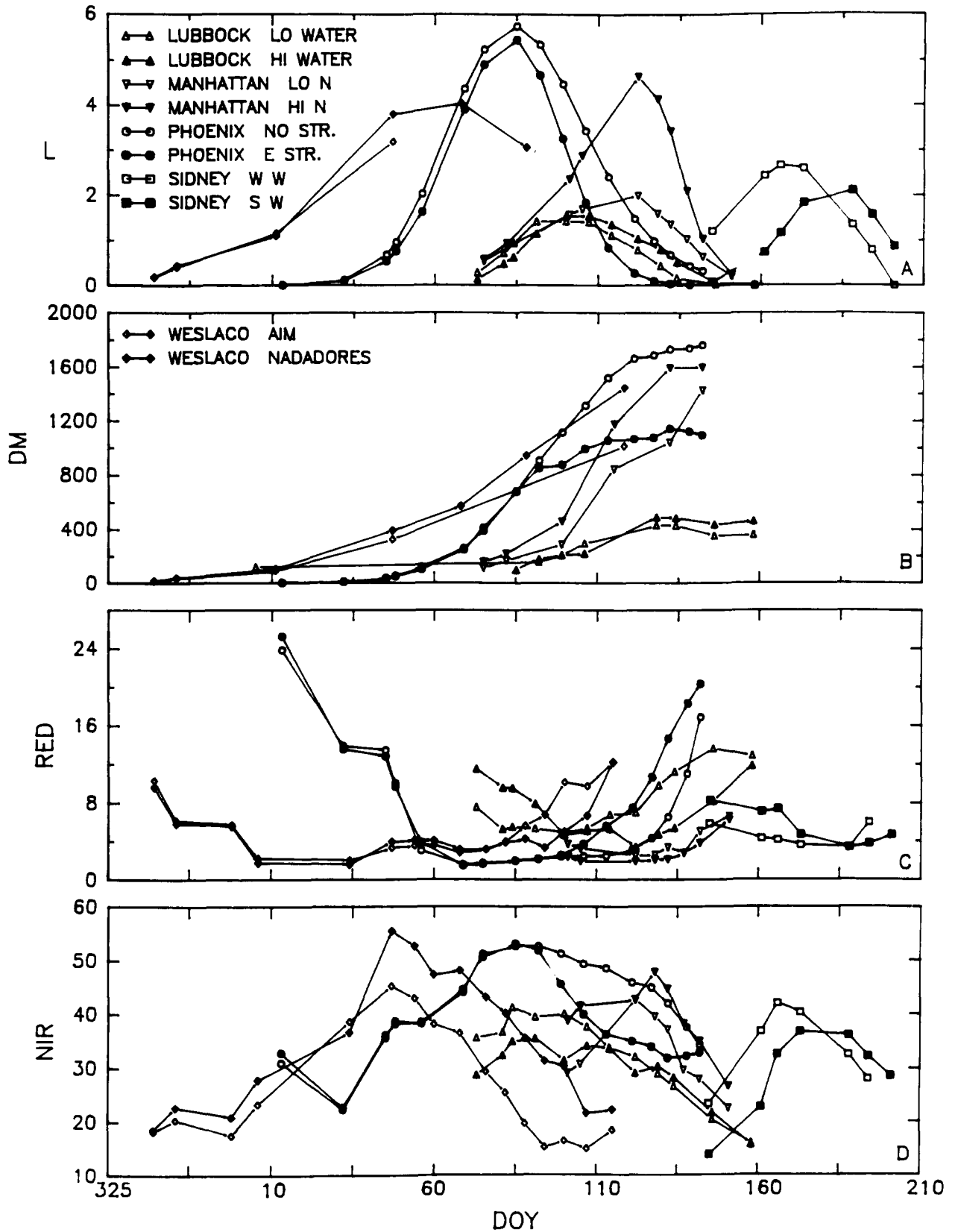


Figure 2. Seasonal leaf area index (L), above-ground dry phytomass (DM), near infrared (NIR), and visible red (RED) reflectance factors for two treatments at each location of this study. DOY is day of year.

lar dry matter accumulation rates as indicated by parallel slopes in Figure 2b were for Phoenix (no stress) versus Manhattan (high nitrogen) and Manhattan (low nitrogen) versus Weslaco (Nadadores). Among locations, dry matter accumulation rates were approximately proportional to L while minimum RED reflectances were generally inversely related to L . Plant and spectral measurements for the winter wheats (WW) grown at Lubbock, Manhattan, and Sidney began after resumption of growth in the spring, so that the soil background effect on early season RED reflectance is most apparent for Phoenix and Weslaco where spectral measurements began prior to or right after emergence.

Within Location Analyses

Vegetation Indices

The relation between L (graphed as the dependent variable) and the four soil-referenced vegetation indices, GVI, TSAVI, PVI, and SAVI2, are shown in Figure 3 by location for the pre- L_{\max} portion of the growing season. Observations are shown by open symbols, the statistical fit to Eq. (9) is shown by closed symbols, and the number of observations is in parentheses. The Sidney data exhibited a higher L for a given vegetation index than the other locations, and the Manhattan data had a higher SAVI2 for $L > 2$ than the other locations. The Lubbock data are distinctive in their tendency to approach asymptotically limiting values of the vegetation indices at $L < 2$. For Phoenix we used data for the cultivar with the most erectophile canopy (Ciano 79), the most planophile canopy (Yecora 70), and two cultivars that had nondistinctive leaf displays (Genaro 81 and Seri 82); data for two other cultivars with nondescript canopies and for the late stress treatment, which had L and spectral responses the same as the no-stress treatment, were deleted to keep the number of observations from this location from dominating the among location analyses.

The within-location analyses of the pre- L_{\max} data were conducted to learn whether agronomic treatments caused the coefficients C , A , and B in Eq. (9) to differ statistically. Briefly, results by location were as follows:

Lubbock. The coefficients C , A , and B did not differ among treatments summarized by cultivar

for any of the VI. There was considerable experimental variation in this data set; the full model form of Eq. (9) explained only 2% more of the variation than the fully reduced form, but neither accounted for over 50% of the variation. The observations of L were erratic, but the large residuals—due, in part, possibly to spectral measurements under windy conditions—were random, so that the data were used.

Phoenix. For SAVI2, NDVI, and TSAVI, C , A , and B did not differ statistically among treatments (two irrigation treatments within each of four cultivars), but C and B differed among treatments for GVI and PVI. The data were very consistent; the fully reduced model (a single C , A , and B for all cultivars and irrigation treatments within a vegetation index) accounted for 95% of the variation in GVI and PVI and for 98% of the variation in SAVI, NDVI, and TSAVI.

In a separate analysis of the individual cultivars using the three irrigation regimes (no, early, and late stress) as treatments, we found that, for GVI, C (the asymptotically limiting value of GVI) was smallest (31.8) and B was largest (0.71) for the erectophile canopy of Ciano, and C was largest (40.4) and B was smallest (0.54) for the planophile canopy of Yecora. Thus, the NIR reflectance was greater for the planophile than the erectophile canopy, but it is improper to compare the absorption-scattering coefficients represented by B when the C 's differ because these two coefficients are strongly inversely correlated. For the ratio indices, SAVI2 and TSAVI, however, C was smallest (14.8 and 0.93, respectively) and B largest (0.32 and 1.14) for the planophile canopy; but for the erectophile canopy C was second largest (at 15.6 and 0.96) and B third smallest (0.29 and 0.95). Thus canopy architecture affects the magnitude of the vegetation indices in seasonal analyses, but the explanation of 95–98% of the variation across cultivars by a single set of coefficients indicates the dominance of the much stronger relation between VI and L .

Manhattan. The C , A , and B did not differ by treatment at the 5% probability level for any of the vegetation indices. The fully reduced model accounted for 78% of the variation in GVI and PVI, 82% of the variation in SAVI, and 92% of the variation in NDVI and TSAVI. The coefficient A differed at the 10% probability level for NDVI and TSAVI.

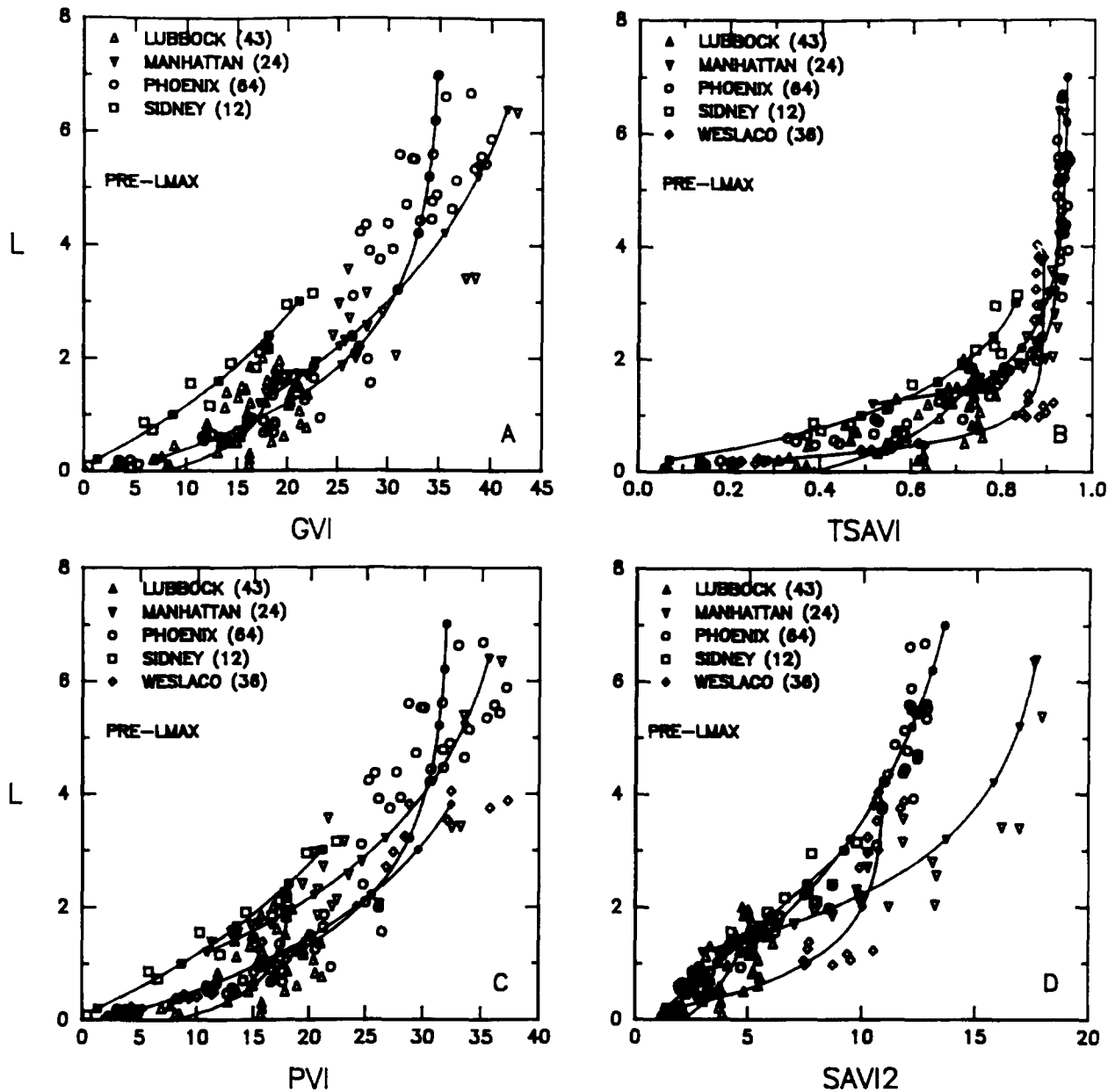


Figure 3. Relation between L and the vegetation indices GVI, TSAVI, PVI, and SAVI2 for the pre- L_{max} portion of the growing season as fit by the fully reduced form of Eq. (9) by location. Observations are shown by open symbols and the statistical fit to Eq. (9) by closed symbols. Number of observations is in parentheses in this figure and the following figures.

Sidney. There were too few observations per treatment for meaningful analysis, so that the data were analyzed as one set using the fully reduced model for each vegetation index. Individual VI accounted for 95–98% of the variation. The relation between L and the VI was nearly linear, causing C to become very large (no asymptotically limiting value of C exists if the data are linear) and, consequently, B to be very small.

Weslaco. The values of C , A , and B did not differ between cultivars for NDVI and TSAVI; but B differed for PVI, and A and B differed for SAVI2. The fully reduced model accounted for 95% of the variation for SAVI2, 97% for PVI, and 98% for NDVI and TSAVI.

The above analyses indicate that cultural treatments did not have a strong effect on the model parameters during the pre- L_{max} portion of

the growing season. The coefficients C , A , and B differed less often among treatments, and the coefficients of determination (R^2) were largest within locations for the ratio vegetation indices SAVI2, NDVI, and TSAVI. On the other hand, the values of the parameter B were statistically different among treatments for the orthogonal vegetation indices, GVI and PVI. Thus, results from this multisite data set summarized by cultivars agrees with the conclusion of Jackson and Pinter (1986) that the orthogonal greenness vegetation indices are more responsive to canopy architectural differences than are ratio vegetation indices. Canopy architectural differences contributed to the uncontrolled variation among sites in this study.

Another source of variation in the data was solar zenith angle (Z). In Figure 4, observed L is plotted against $L_z = L / \cos Z$ for pre- L_{\max} and post- L_{\max} portions of the season. The deviation from the 1:1 line is large for Sidney during both portions of the season because of the early morning measurements and the high latitude of the site. At Weslaco, pre- L_{\max} observations were made from mid-December to mid-February when the sun was low in the sky. Observations at Phoenix were made about 2 h prior to solar noon throughout the season and pre- L_{\max} data ranged in time from 13 January to 27 March. Solar zenith angles were smallest for Lubbock and Manhattan (pre- L_{\max}) and those two sites and Phoenix (post- L_{\max}). The solar zenith angle differences summarized in Figure 4, any errors in determining the soil lines (Fig. 1), and differences due to instruments would all contribute variation in the calculated vegetation indices.

Fractional PAR Absorbed (FPAR)

Application of Eq. (9) and the F-tests to the Manhattan '83 pre- L_{\max} FPAR data (Lapitan, 1986) showed that the fully reduced model in which $C = 1.00$, $A = 0.91 \pm 0.08$, and $B = 0.86 \pm 0.12$ was appropriate. That is, the asymptotic limit of FPAR was unity as L became very large, whereas light transmission at $L = 0$ was estimated to be 0.91, and the absorption-scattering coefficient in the PAR wavelengths, B , was 0.86.

For the Weslaco FPAR data, the appropriate model was one, in which C was 1.00, $A = 0.93 \pm 0.05$, and $B = 0.93 \pm 0.08$. The respective coefficients for the two locations were very similar, so

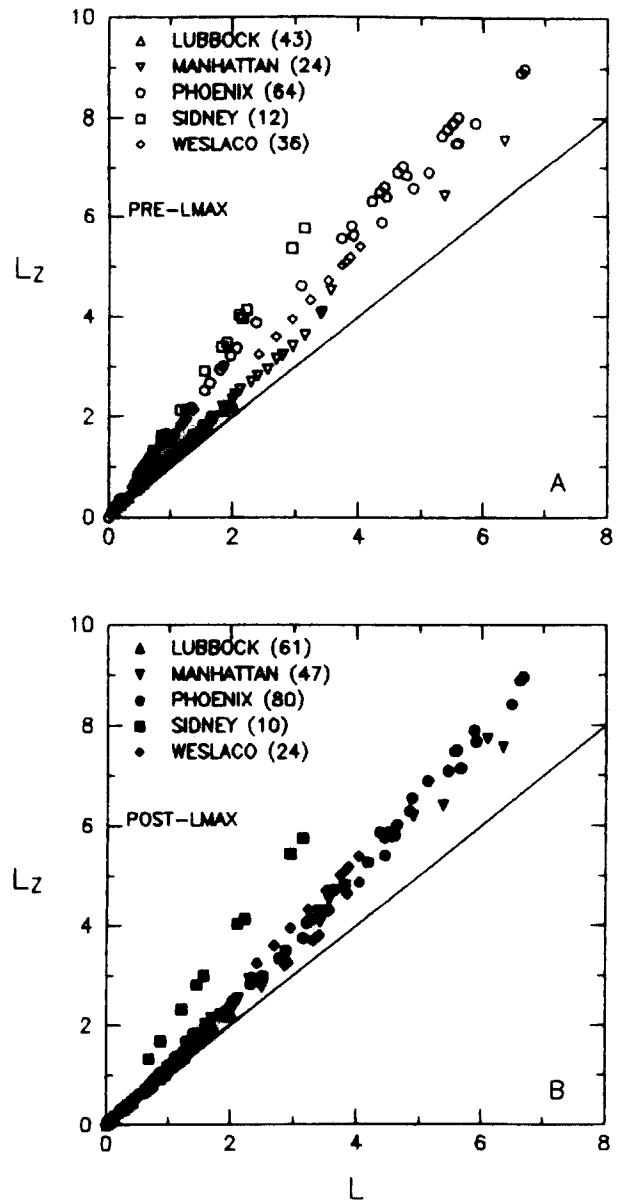


Figure 4. Relation between L and $L_z = L / \cos$ (solar zenith angle) for pre- L_{\max} and post- L_{\max} portions of the growing season by location.

that the data are analyzed as one set in the following section.

Among Location Analyses

L Estimated from VI

The data pooled for all sites are summarized in Figure 5 and the equations and statistical parameters for the pre- L_{\max} , post- L_{\max} , and whole season periods are given in Tables 4, 5, and 6, respec-

Table 4. Across Location Equations for the Pre- L_{\max} Portion of the Growing Season

Equations (by Form)		R^{2a}	RMSE	S_b	Eq. No.	
1. $L =$	$-1.124 + 0.153(\text{GVI})$	0.78	0.80	0.007	(10)	
	$= -0.901 + 0.159(\text{PVI})$	0.78	0.77	0.006	(11)	
	$= 0.094 + 0.154(\text{RVI})$	0.81	0.72	0.006	(12)	
	$= -0.484 + 0.372(\text{SAVI2})$	0.81	0.72	0.013	(13)	
	$= -1.782 + 5.217(\text{NDVI})$	0.56	1.10	0.346	(14)	
	$= -1.147 + 4.563(\text{TSAVI})$	0.56	1.10	0.301	(15)	
2. $L =$	$0.381 \exp[0.070(\text{GVI})]$	0.82	0.74	0.003	(16)	
	$= 0.369 \exp[0.079(\text{PVI})]$	0.84	0.67	0.003	(17)	
	$= 0.831 \exp[0.057(\text{RVI})]$	0.72	0.87	0.003	(18)	
	$= 0.707 \exp[0.134(\text{SAVI2})]$	0.70	0.91	0.007	(19)	
	$= 0.006 \exp[7.085(\text{NDVI})]$	0.80	0.74	0.448	(20)	
	$= 0.013 \exp[6.256(\text{TSAVI})]$	0.80	0.74	0.391	(21)	
3. $L =$	$0.036 + 0.0047(\text{GVI}) + 0.0036(\text{GVI})^2$	0.85	0.68	—	(22)	
	$= 0.110 - 0.0004(\text{PVI}) + 0.0045(\text{PVI})^2$	0.86	0.63	—	(23)	
	$= 1.682 - 9.7129(\text{NDVI}) + 12.879(\text{NDVI})^2$	0.73	0.86	—	(25)	
	$= 0.814 - 6.2754(\text{TSAVI}) + 10.284(\text{TSAVI})^2$	0.73	0.85	—	(26)	
4. $L =$	$0.0051(\text{GVI} \cdot 1.914)^b$	0.85	0.68	0.090	(27)	
	$= 0.0064(\text{PVI} \cdot 1.905)$	0.86	0.63	0.077	(28)	
	$= 0.2139(\text{RVI} \cdot 0.905)$	0.82	0.71	0.043	(29)	
	$= 0.1798(\text{SAVI2} \cdot 1.246)$	0.81	0.73	0.062	(30)	
	$= 6.560(\text{NDVI} \cdot 6.056)$	0.79	0.77	0.416	(31)	
	$= 6.385(\text{TSAVI} \cdot 5.272)$	0.79	0.76	0.353	(32)	
5. Fully reduced three-parameter model						
	C	A	B	R^2	RMSE	Eq. No.
GVI	41.01 ± 2.54	0.852 ± 0.017	0.329 ± 0.049	0.84	4.05	(9a)
PVI	37.02 ± 2.26	0.873 ± 0.015	0.335 ± 0.047	0.83	3.79	(9b)
RVI	75.78 ± 28.27	0.992 ± 0.007	0.089 ± 0.042	0.82	4.16	(9c)
SAVI2	16.90 ± 1.41	0.939 ± 0.013	0.259 ± 0.041	0.85	1.54	(9d)
NDVI	0.91 ± 0.01	0.773 ± 0.021	1.225 ± 0.089	0.87	0.09	(9e)
TSAVI	0.90 ± 0.02	0.890 ± 0.024	1.202 ± 0.087	0.90	0.10	(9f)

^a (Total corrected sum of squares – residual sum of squares)/(total corrected sum of squares).

Applies also to Tables 5 and 6.

^b Double asterisks mean “raised to the power” here and in Tables 5 and 6.

tively. In Figure 5 the data are displayed for the four vegetation indices that are referenced to the soil, whereas results in the tables also include equations for the two vegetation indices RVI and NDVI, which are not referenced to the soil. The equations displayed in Figure 5 for the pre- and post- L_{\max} portions of the season are those that gave the highest coefficient of determination (R^2) in Tables 4 and 5. The best fit for GVI was quadratic, for TSAVI exponential, for PVI a power, and for SAVI2 linear.

Statistical t-tests for the linear equations for SAVI2 in Figure 5 showed that the slopes did not differ statistically at the 0.05 probability level for the pre- L_{\max} and post- L_{\max} equations and that the corresponding intercepts both differed significantly from zero. Therefore, Eq. (13b) in Table 6 for the whole season can be recommended; the

root mean square error (RMSE) is smaller than for either seasonal portion because of the effect of the number of observations on the calculation of RMSE. Statistical tests of the slopes and intercepts of the linear equations for RVI in Tables 4, 5, and 6 indicate that Eq. (12b), Table 6, describes the RVI data well.

Although the quadratic equation gave the highest coefficient of determination during both pre- L_{\max} and post- L_{\max} portions of the season only for GVI, the quadratic terms contributed significantly (0.05 level) during both these seasonal parts for all the VI except RVI and SAVI2. For the whole season the quadratic term contributed significantly for SAVI2 but not for RVI. Consequently, the quadratic equation was included for SAVI2 only in Table 6.

The significance of the quadratic term for the

Table 5. Across Location Equations for the Post- L_{\max} Portion of the Growing Season

Equations (by Form)				R^2	RMSE	S_b	Eq. No.
1.	$L = -1.137 + 0.137(\text{GVI})$			0.68	0.95	0.007	(10a)
	$= -1.078 + 0.152(\text{PVI})$			0.66	0.98	0.007	(11a)
	$= -0.277 + 0.186(\text{RVI})$			0.77	0.82	0.007	(12a)
	$= -0.730 + 0.383(\text{SAVI2})$			0.72	0.90	0.016	(13a)
	$= -1.913 + 5.074(\text{NDVI})$			0.45	1.26	0.379	(14a)
	$= -1.328 + 4.468(\text{TSAVI})$			0.45	1.26	0.333	(15a)
2.	$L = 0.193 \exp[0.088(\text{GVI})]$			0.80	0.75	0.004	(16a)
	$= 0.233 \exp[0.091(\text{PVI})]$			0.75	0.85	0.004	(17a)
	$= 0.692 \exp[0.071(\text{RVI})]$			0.69	0.95	0.003	(18a)
	$= 0.591 \exp[0.149(\text{SAVI2})]$			0.63	1.03	0.008	(19a)
	$= 0.0006 \exp[9.691(\text{NDVI})]$			0.75	0.85	0.627	(20a)
	$= 0.002 \exp[8.524(\text{TSAVI})]$			0.74	0.86	0.561	(21a)
3.	$L = 0.300 - 0.056(\text{GVI}) + 0.0048(\text{GVI})^2$			0.80	0.76	—	(22a)
	$= 0.164 - 0.0305(\text{PVI}) + 0.0050(\text{PVI})^2$			0.74	0.86	—	(23a)
	$= 1.925 - 11.862(\text{NDVI}) + 14.821(\text{NDVI})^2$			0.65	1.01	—	(25a)
	$= 0.667 - 6.959(\text{TSAVI}) + 11.037(\text{TSAVI})^2$			0.64	1.02	—	(26a)
4.	$L = 0.0006(\text{GVI} \cdot 2.514)$			0.80	0.75	0.125	(27a)
	$= 0.002(\text{PVI} \cdot 2.231)$			0.74	0.86	0.123	(28a)
	$= 0.105(\text{RVI} \cdot 1.159)$			0.77	0.82	0.058	(29a)
	$= 0.106(\text{SAVI2} \cdot 1.452)$			0.72	0.89	0.081	(30a)
	$= 8.425(\text{NDVI} \cdot 8.358)$			0.74	0.87	0.572	(31a)
	$= 7.970(\text{TSAVI} \cdot 7.228)$			0.73	0.88	0.508	(32a)
5. Fully reduced three-parameter model							
	C	A	B	R^2	RMSE		Eq. No.
GVI	38.60 ± 1.95	0.789 ± 0.018	0.423 ± 0.059	0.76	5.02		(9q)
PVI	37.50 ± 3.15	0.771 ± 0.020	0.303 ± 0.062	0.70	4.99		(9h)
RVI	65.25 ± 27.0	0.953 ± 0.082	0.082 ± 0.043	0.77	3.85		(9i)
SAVI2	16.33 ± 1.84	0.854 ± 0.016	0.235 ± 0.052	0.75	1.89		(9j)
NDVI	0.90 ± 0.02	0.571 ± 0.021	1.201 ± 0.144	0.69	0.13		(9k)
TSAVI	0.89 ± 0.02	0.654 ± 0.024	1.194 ± 0.144	0.68	0.14		(9l)

Table 6. Across Location Equations for the Whole Season (Combined Pre- and Post- L_{\max} Portions of the Season)

Equations (by Form)	R^2	RMSE	S_b	Eq. No.
1. $L = -1.048 + 0.137(\text{GVI})$	0.71	0.87	0.005	(10b)
$= -0.892 + 0.146(\text{PVI})$	0.69	0.89	0.005	(11b)
$= -0.096 + 0.165(\text{RVI})$	0.78	0.74	0.005	(12b)
$= -0.612 + 0.372(\text{SAVI2})$	0.76	0.78	0.011	(13b)
$= -1.665 + 4.739(\text{NDVI})$	0.49	1.13	0.254	(14b)
$= -1.104 + 4.159(\text{TSAVI})$	0.49	1.13	0.222	(15b)
2. $L = 0.240 \exp[0.083(\text{GVI})]$	0.80	0.72	0.003	(16b)
$= 0.268 \exp[0.088(\text{PVI})]$	0.76	0.77	0.003	(17b)
$= 0.726 \exp[0.063(\text{RVI})]$	0.69	0.89	0.002	(18b)
$= 0.573 \exp[0.152(\text{SAVI2})]$	0.67	0.91	0.006	(19b)
$= 0.002 \exp[8.409(\text{NDVI})]$	0.76	0.77	0.402	(20b)
$= 0.004 \exp[7.415(\text{TSAVI})]$	0.76	0.77	0.357	(21b)
3. $L = 0.223 - 0.037(\text{GVI}) + 0.0045(\text{GVI})^2$	0.80	0.71	—	(22b)
$= 0.162 - 0.020(\text{PVI}) + 0.0048(\text{PVI})^2$	0.77	0.77	—	(23b)
$= -0.363 - 0.271(\text{SAVI2}) + 0.0070(\text{SAVI})^2$	0.77	0.77	—	(24)
$= 1.663 - 9.934(\text{NDVI}) + 12.88(\text{NDVI})^2$	0.67	0.91	—	(25b)
$= 0.692 - 6.095(\text{TSAVI}) + 9.933(\text{TSAVI})^2$	0.67	0.91	—	(26b)
4. $L = 0.0014(\text{GVI} \cdot 2.259)$	0.81	0.71	0.084	(27b)
$= 0.0033(\text{PVI} \cdot 2.082)$	0.77	0.77	0.080	(28b)
$= 0.1445(\text{RVI} \cdot 1.032)$	0.78	0.74	0.038	(29b)
$= 0.117(\text{SAVI2} \cdot 1.415)$	0.77	0.77	0.055	(30b)
$= 7.184(\text{NDVI} \cdot 7.234)$	0.75	0.79	0.371	(31b)
$= 6.897(\text{TSAVI} \cdot 6.283)$	0.75	0.80	0.327	(32b)

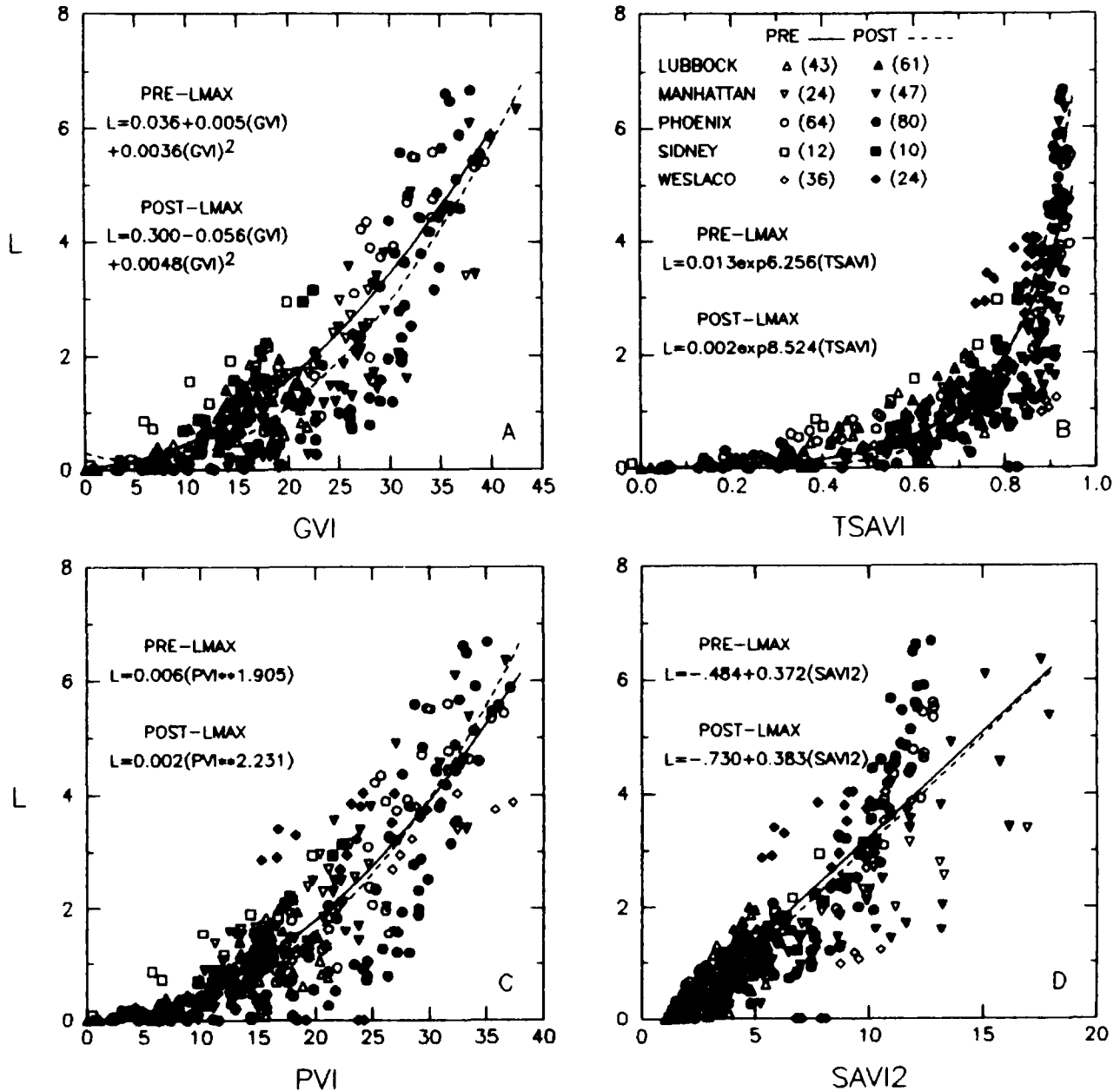


Figure 5. Data for all locations pooled and the equations that describe the data by pre- L_{\max} (open symbols) and post- L_{\max} (closed symbols) portions of the season.

indices PVI, NDVI, and SAVI2 is a clue that exponential or power equation forms might best relate those indices to L . In selecting the exponential equation form to represent TSAVI and the power form to represent PVI in Figure 5, we chose the equation form that had the best combination of high R^2 and low RMSE during both seasonal portions. The RMSE in estimating L during the pre- L_{\max} period ranged from 0.63 for

PVI to 0.74 for TSAVI using the equation forms in Figure 5.

For the post- L_{\max} period and the equation forms of Figure 5, the RMSE ranged from 0.76 for GVI to 0.90 for TSAVI. Interestingly, for the whole season data (Table 6), the equation form used in Figure 5 estimated L with a RMSE of 0.71 for GVI while for the other three indices RMSE was 0.77–0.78.

The single equation form that best described $L(VI)$ across all vegetation indices and growing season portions was the power equation form. It placed no lower than second for any of the six vegetation indices using the R^2 and RMSE criteria mentioned. By comparison, for corn (Wiegand et al., 1990) the power equation form described all the two-band vegetation indices well but not the three- and four-band greenness vegetation indices. For the wheat data of this study, this versatile equation form also described the GVI data as well as the quadratic equation did.

The coefficients of the three-parameter (or coefficient) model for estimating the VI from L across all locations are given in the last section in Tables 4 and 5. For the pre- L_{\max} portion of the season, this equation form gave the highest R^2 for NDVI and TSAVI and estimated NDVI with a RMSE of 0.09 [Table 4, Eqs. (9e) and (9f)]. The three-parameter model is not appropriate for data that are essentially linear (no asymptotically limiting value of C exists) as $RVI(L)$ usually is. Thus the iterative procedure either fails to converge on values of C and B or arrives at unrealistically large values of C that are offset by unrealistically small values of B , both of which are uncertain. That happened for the RVI fits expressed by Eq. (9c) in Table 4 and Eq. (9i) in Table 5.

The modification of RVI to account for soil, SAVI2, performed better than RVI only in the three-parameter model for the pre- L_{\max} portion of the season. Consequently, soil was a weak source of experimental variation, compared with other sources of variation, during the post- L_{\max} part of the season, since the modification of the data expressed by Eq. (6), compared with Eq. (5), was ineffective.

The equation forms shown in Figure 5 agree well with those recommended for corn (Wiegand et al., 1990). For corn, a linear equation was best for RVI, the exponential form was the choice for NDVI, a quadratic equation best fit GVI, and power, linear, or quadratic equation forms were equally applicable for PVI. The coefficients of determination for corn were several hundredths higher during the pre- L_{\max} portion of the season than during the post- L_{\max} part of the season in agreement with the findings for wheat in this study.

FPAR Estimated from L and L_z

The fractional PAR absorbed data from Manhattan and Weslaco were related to L and to L_z using

SAS nonlinear procedures and Eq. (9). However, whenever C or A did not differ from unity, they were deleted, and the data were refit to an equation with fewer coefficients. The extinction coefficient (B) depends on both solar zenith angle (Z) and leaf angle distribution, so that use of $L_z = L / \cos Z$ should make extinction coefficients obtained at sites that differ in latitude and growing seasons more comparable. Measurements at Weslaco were made from January to March and at Manhattan from March to May, so that solar zenith angles were greater for Weslaco than for Manhattan (Fig. 4). For the combined data set neither C nor A differed from unity and the equations,

$$\begin{aligned} \text{FPAR} &= 1 - \exp[-1.00(L)], \\ r^2 &= 0.952, \quad \text{RMSE} = 0.054 \end{aligned} \quad (33)$$

and

$$\begin{aligned} \text{FPAR} &= 1 - \exp[-0.679(L_z)], \\ r^2 &= 0.942, \quad \text{RMSE} = 0.059 \end{aligned} \quad (34)$$

were obtained. The data that produced Eq. (33) are displayed in Figure 6. Compared with the observations, Eq. (33) overestimates FPAR for $L > 3$.

FPAR Estimated from VI

If FPAR can be estimated from VI, then the need for L is lessened because one of the main uses of L is to estimate FPAR. FPAR could be estimated from the combined GVI data for Manhattan and PVI data for Weslaco by the equation given in Figure 7a and from SAVI2 by the equation given in Figure 7b. For Manhattan, GVI and PVI were almost the same magnitude (mean GVI = 13.48 and mean PVI = 13.24) so that there would be little change in the equation had it been expressed in terms of PVI.

The Manhattan and Weslaco data differed in the relation between VI and L , and so in the FPAR(VI) relation. For the Weslaco data alone, the equations for FPAR estimated from NDVI, RVI, and PVI were:

$$\begin{aligned} \text{FPAR} &= -0.450 + 1.449(\text{NDVI}), \\ R^2 &= 0.72, \quad \text{RMSE} = 0.13, \end{aligned} \quad (35)$$

$$\begin{aligned} \text{FPAR} &= 0.173(\text{RVI}^{**0.573}) \\ R^2 &= 0.77, \quad \text{RMSE} = 0.12, \end{aligned} \quad (36)$$

and

$$\begin{aligned} \text{FPAR} &= 0.109(\text{PVI}^{**0.666}) \\ R^2 &= 0.88, \quad \text{RMSE} = 0.09. \end{aligned} \quad (37)$$

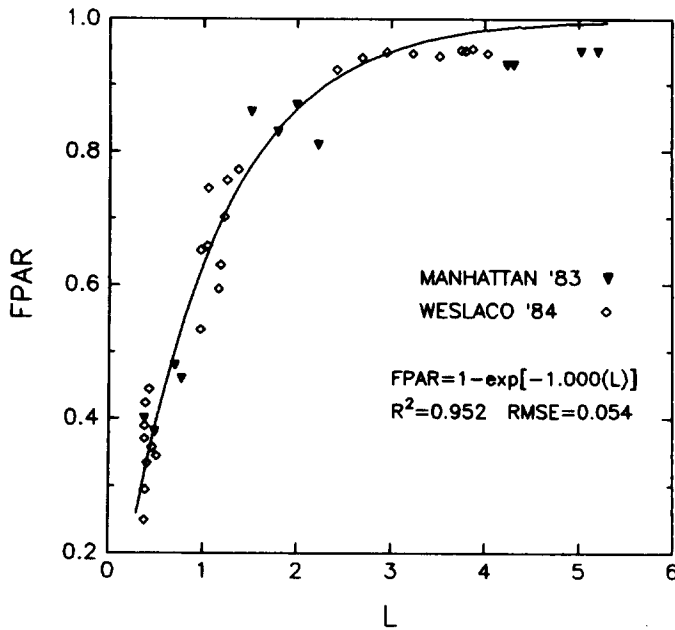


Figure 6. FPAR estimated from L for the combined Manhattan '83 and Weslaco '84 measurements.

The above equations from Weslaco differ from those previously published (Table 8C) because data points for a third cultivar, Yavaros, were deleted here. Equations for the Manhattan data (Lapitan, 1986), 0.36 m row spacing, are summarized in table 8C.

DISCUSSION

Apprehension about the data of this study concerned interlocation variation in sun angle, soils, instruments and technique, and leaf angle distributions. We attempted to eliminate large experimental errors by deleting whole data sets when errors in processing were indicated and emphasizing vegetation indices referenced to the soil to minimize partial cover effects. However, we deliberately included data from Phoenix for cultivars with very erectophile and very planophile canopy architectures to encompass the full range in leaf displays available in the data.

Soil brightness effects on vegetation indices not accounted for in referencing them to the soil and errors in positioning the soil lines also contribute experimental error. For example, a soil line,

$$\text{NIR} = 3.11 + 1.172(\text{RED}), \quad (38)$$

was extracted for Phoenix from observations in

the data set prior to emergence of the wheat, but it was somewhat imprecise ($r^2 = 0.90$) because it represented only dry and cloddy soil. The slope, 1.064, of the soil line used for Phoenix (numbered 3 in Fig. 1) is lower than those for other sites and those for other MMR data given in Wiegand et al. (1990). Error in determining soil lines affects soil-referenced vegetation indices and, consequently, the equation coefficients in relations involving them. This source of error is small.

The largest sources of variation in the data concern measurement of L and observations of reflectance factors under differing sun angles and vegetation ground cover conditions among experimental sites. In spite of these sources of variation, the data displayed in Figure 5 and the measures of goodness of fit for the equations of Tables 4, 5, and 6 indicate that L can be estimated with a RMSE between 0.7 and 0.8 from each of the vegetation indices by at least one equation form. The lowest RMSE, 0.63, and the highest R^2 , 0.86, were obtained during the pre- L_{\max} portion of the season for L expressed as a power or as a quadratic function of PVI (Table 4). These results are comparable to those reported (Goel, 1988) for estimating L by inverting the scattering by arbitrarily inclined leaves (SAIL) model (Verhoef, 1984), even though those applications have mostly been to diurnal data from one location, not seasonal data from multiple sites as here.

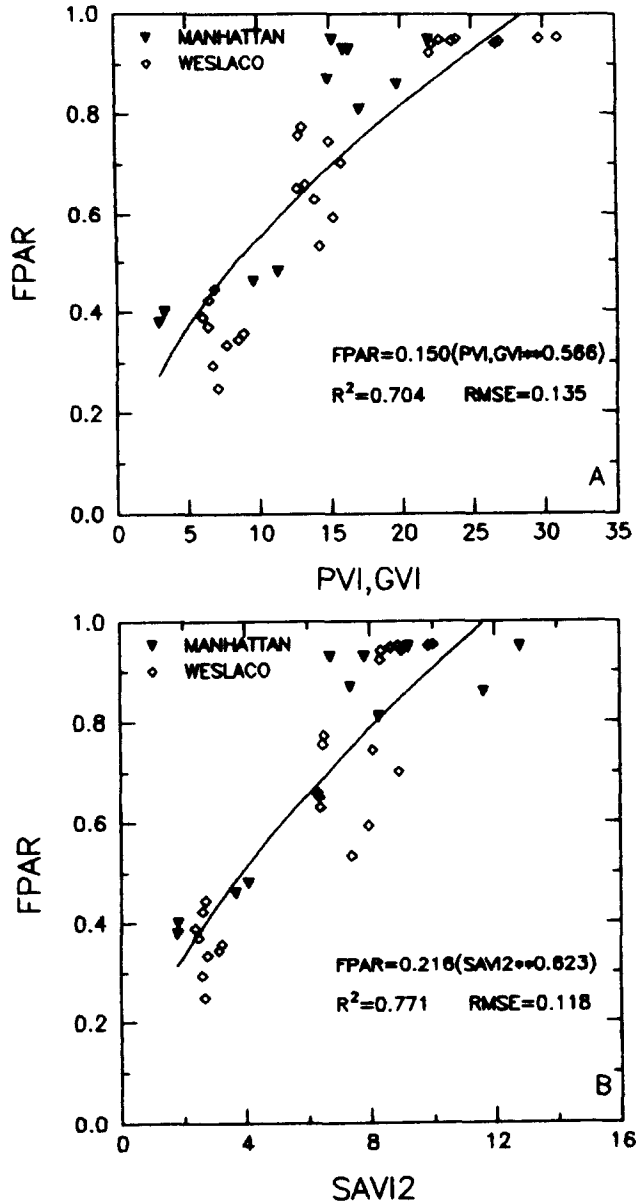


Figure 7. FPAR estimated from the combined GVI data from Manhattan and the PVI data from Weslaco, and from SAVI2 for both locations.

In the pre- L_{\max} portion of the season, the VI estimates were improved for ratio vegetation indices referenced to the soil line. The implications of this finding are that a) other canopy characteristics, such as content of nonliving tissue or presence of heads, are reducing the information extractable about soil-adjusted vegetation indices during the post- L_{\max} portion of the season, or, alternatively, b) variations in soil brightness among locations were a detectable source of variation within vegetation indices.

Huete (1989) separated the soil influences on vegetation indices into brightness (or reflectance magnitude) and shape (or soil line slope) effects as these interact with vegetation cover and sun angle in influencing vegetation indices. Generally, ratio vegetation indices decrease for a constant L the more reflective the soil, whereas the orthogonal indices GVI and PVI increase as soil reflectance increases. In his studies, the vegetation index response to light and dark soil backgrounds as L increased was in the order $\text{SAVI} < \text{PVI} < \text{NDVI}$. Huete (1989) described the slope of the vegetation isolines in red and near-infrared 2-space, M_{vi} , by the equation

$$M_{vi} = a \exp[2(k_{\text{RED}} - k_{\text{NIR}})L], \quad (39)$$

wherein a is the slope of the soil line as in Eq. (3), and k_{RED} and k_{NIR} are canopy extinction coefficients in RED and NIR wavelengths. For photosynthetically active canopies $k_{\text{RED}} > k_{\text{NIR}}$, and M_{vi} increases as L increases because the soil reflects the NIR flux scattered by the canopy while little RED flux reaches the soil. If k_{RED} and k_{NIR} were the same for the cultivars at the different locations and for the wavelengths of the radiometers used in this study, the slope of the vegetation isolines would be proportional to the slope of the soil lines.

All vegetation indices are affected by solar zenith angle. Since canopies of live, green vegetation are less reflective than most agricultural soils in the RED and more reflective than the soil background in the NIR, at partial ground cover, canopy reflectance is higher in the RED and lower in the NIR the smaller the solar zenith angle. However, for particular combinations of sun angle, L , and soil background reflectance, the indices can increase, decrease, or be unchanged (Huete, 1989).

In this study, sun angle, plant cover, canopy architecture, amount of photosynthetically inactive tissue in the canopies, errors in measurements, and soil reflectance all varied among sites so that it is not surprising that the two vegetation indices (SAVI2 and TSAVI) that adjust for soil brightness were not superior for estimating L (Tables 4, 5, and 6) in any part of the season. In spite of these complications up to 86% of the variation in L and up to 90% of the variation in vegetation indices was accounted for during the pre- L_{\max} part of the season. Thus the vegetation indices are robust in distinguishing photosyntheti-

Table 7. Values of the VI_g Terms of Eq. (40) for the Soils and Vegetation Indices of This Study

Location	Soil Condition	GVI_g	PVI_g	RVI_g	$SAVI2_g$	$NDVI_g$	$TSAVI_g$
Lubbock	Wet	1.44	1.34	1.49	1.20	0.20	-0.01
	Dry	1.44	1.34	1.37	1.23	0.15	0.01
Manhattan, '85	Wet	1.30	1.25	1.61	1.28	0.23	-0.01
	Dry	1.30	1.25	1.44	1.28	0.18	0.00
Phoenix	Wet	2.35	1.74	1.24	1.06	0.11	0.00
	Dry	2.35	1.74	1.15	1.06	0.07	0.00
Sidney	Wet	0.72	0.89	1.58	1.40	0.23	0.00
	Dry	0.72	0.89	1.48	1.40	0.19	0.00
Weslaco	Wet	—	0.41	1.65	1.30	0.25	-0.04
	Dry	—	0.41	1.48	1.28	0.19	-0.02
Manhattan, '83	Wet	-0.24	0.32	1.49	1.44	0.20	0.00
	Dry	-0.24	0.32	1.46	1.44	0.19	0.00

cally active canopies from the soil backgrounds and in quantifying them even in the presence of the real world complications. Taken together our results force the conclusion that the green leaf area index of the wheat canopies strongly dominated the reflectance factor observations. Consequently, it was possible to develop generalized equations to recommend for predicting L and fractional photosynthetically active radiation absorption for wheat from spectral observations expressed as vegetation indices.

Equations that are at least semitheoretical have been derived for relating vegetation indices and L or FPAR. They include the equation (Baret and Guyot, 1991),

$$VI = VI_{\infty} + (VI_g - VI_{\infty}) \exp(-K_{vi} * L), \quad (40)$$

which is directly analogous to Eq. (9) in form and interpretation when one lets $C = VI_{\infty}$, $A * C = (VI_g - VI_{\infty})$, and $B = K_{vi}$. Consequently, the values of VI_{∞} are given by the values of C at the bottom of Tables 4 and 5 for the data pooled across all sites and the six vegetation indices of this study. The values of VI_g for each vegetation index and location of this study are summarized in Table 7. RVI_g , $SAVI2_g$, $NDVI_g$, and $TSAVI_g$ were calculated from the data for the soil lines of Figure 1 using the equations in Table 3. GVI_g and PVI_g are opposite in sign to the intercepts in the equations for these indices in Table 3. From experience and the literature the slope of most soil lines expressed as in Figure 1 is about 1.2 for the MMR and 1.4 for the EXO 100A, and $NDVI$ of agricultural soils

devoid of vegetation is usually 0.20 ± 0.05 . The small slope, 1.06, for Phoenix caused $NDVI_g$, as well as RVI_g and $SAVI2_g$, to fall outside the usual range. Thus Eq. (38) may have represented the Avondale soil at Phoenix better than the equation given in Figure 1.

Sellers (1987) and Choudhury (1987) both used a two-stream approximation of the radiative transfer equation to investigate the relation between FPAR and RVI , and FPAR and $NDVI$, respectively. Sellers concluded that the relation between FPAR and RVI , controlled by NIR-scattering properties of the leaves, is nearly linear for dark soils and becomes increasingly nonlinear as the soil reflectance increases. One of Sellers' assumptions, to simplify the analysis, was that the soil reflectance is the same in both RED and NIR wavelength intervals. Choudhury found the relation between $NDVI$ and FPAR was curvilinear but that changes in soil reflectance affected it. Unfortunately, neither investigator fit the displayed data by an equation so that the theoretical results cannot be compared with the empirical equations of this study. Reflectance of the soil background is difficult to specify for particular times of interest during a growing season under field conditions because of periodic cultivation, irrigation, and rainfall. Consequently, in estimating L by inverting the SAIL model soil reflectance is also often the least certain parameter (Goel, 1988).

Wiegand and Richardson (1984; 1987) presented the identity

$$FPAR(VI) = L(VI) \times FPAR(L), \quad (41)$$

for interrelating FPAR (decimal fraction), VI and L . Empirical functional relationships reported for wheat for each term in Eq. (41) are summarized in Table 8, where all vegetation indices are based on reflectance factors and no distinction is made whether FPAR is fractional intercepted or absorbed photosynthetically active radiation since authors used them interchangeably. (Intercepted = $1 - T$ whereas absorbed = $1 - T - R_c + TR_s$, where T = transmittance of the canopy, R_c = reflectance of the canopy, and R_s = reflectance of the soil.) Only a few relations between FPAR and L for wheat could be found in the remote sensing literature and the non-remote-sensing literature was briefly searched unsuccessfully. The relation obtained here [Eq. (33), Fig. 6] agrees well, however, with the data of Hipps et al. (1983) and Asrar et al. (1984) in Table 8. Hipps et al. (1983) stated that their equation would overestimate intercepted

PAR by 0.08 to 0.10 at low L on clear days, while Figure 6 shows that the equation of this study overestimates FPAR by a few hundredths at $L > 3$.

Part B of Table 8 contains estimates of L from five vegetation indices, but one should consult the references for specific wavelengths, characteristics of the data, and procedures used to calculate the VI before making comparisons. For example, the L data of Hinzman et al. (1986) were well distributed between $L = 1$ and 4, but the only data below $L = 0.8$ is evidently for bare soil. GVI was calculated from the three visible and three reflective infrared bands of the Thematic Mapper, but 30 was arbitrarily added to the GVI equation "to assure positive values for bare soil." Consequently, the slope, 0.068, for their relation is much lower than the 0.114 reported by Hatfield et al. (1985) and the 0.206 of Dusek et al. (1985). The GVI of Dusek et al. (1985) are based on Bands 1, 2, and

Table 8. Functional Relations from the Literature between A) FPAR (Decimal Fraction) and L , B) L and Vegetation Indices (VI), and C) FPAR and L^a

Functional Relation	R^2	Reference
A. FPAR (decimal fraction) as a function of L:		
FPAR = $0.935[1 - \exp(-0.91L)]$, spring green – up to soft dough	0.99	Hipps et al. (1983)
FPAR = $0.935[1 - \exp(-0.90L)]$, pre- L_{\max}	?	Asrar et al. (1984)
= $0.935[1 - \exp(-0.2 \exp(-0.95 L))]$, post- L_{\max}	?	Asrar et al. (1984)
FPAR = $1 - 0.788 \exp(-0.768L)$	0.94	Wiegand and Richardson (1990)
B. Leaf area index (L) as a function of vegetation indices:		
$L = -0.581 + 0.319(\text{RVI})$	0.87	Kanemasu et al. (1985)
$L = -0.36 + 0.285(\text{RVI})$, pre- L_{\max}	0.86	Hatfield et al. (1985)
= $-0.52 + 0.281(\text{RVI})$, post- L_{\max}	0.84	Hatfield et al. (1985)
= $-0.636 + 0.114(\text{GVI})$, pre- L_{\max}	0.76	Hatfield et al. (1985)
= $-1.46 + 0.145(\text{GVI})$, post- L_{\max}	0.71	Hatfield et al. (1985)
$L = -0.609 + 0.239(\text{PVI})$	0.82	Dusek et al. (1985)
= $-0.631 + 0.206(\text{GVI})$	0.82	Dusek et al. (1985)
$L = 0.273 + 0.149(\text{RVI})$	0.76	Hinzman et al. (1986)
= $-0.10 + \exp[-3.047 + 4.625(\text{NDVI})]$	0.92	Hinzman et al. (1986)
= $-1.604 + 0.0683(\text{GVI})$	0.82	Hinzman et al. (1986)
$L = 2.381 \ln[(0.90 / (0.90 - \text{TSAVI}))]^b$?	Baret et al. (1989)
$L = 0.011 \exp(5.92 \text{ NDVI})$	0.71	Wiegand and Richardson (1990)
= $0.199 \exp(0.094 \text{ PVI})$	0.94	Wiegand and Richardson (1990)
C. FPAR as a function of VI:		
FPAR = $-0.109 + 1.253(\text{NDVI})$	0.96	Asrar et al. (1984)
FPAR = $-0.010 + 0.0218(\text{GVI})$, pre- L_{\max}	0.92	Hatfield et al. (1984)
= $+0.690 + 0.0055(\text{GVI})$, post- L_{\max}	0.84	Hatfield et al. (1984)
= $-0.188 + 1.210(\text{NDVI})$, pre- L_{\max}	0.97	Hatfield et al. (1984)
= $0.595 + 0.369(\text{NDVI})$, post- L_{\max}	0.89	Hatfield et al. (1984)
FPAR = $-0.040 + 1.157(\text{NDVI})$	0.94	Lapitan (1986), pp. 108 and 110,
= $0.962[1 - 1.547 \exp(-0.348 \text{ RVI})]$?	0.36 m row spacing.
= $0.969[1 - \exp(-9.934 \text{ GVI})]$?	
FPAR = $1.205(\text{TSAVI})$	0.95	Baret et al. (1989)
FPAR = $-0.724 + 1.76(\text{NDVI})$	0.76	Wiegand and Richardson (1990)
= $0.184 + 0.025(\text{PVI})$	0.85	Wiegand and Richardson (1990)

^a No distinction is made between "intercepted" and "absorbed" photosynthetically active radiation in defining FPAR, and all vegetation indices are based on reflectance factors.

^b Authors' Eq. (12) solved for L as dependent variable.

4 of the Barnes MMR (Table 2), but those of Hatfield et al. (1985), on the four bands of the Exotech 100A (Table 2) using greenness equation coefficients from the literature. Vegetation indices approach limiting values asymptotically as L increases (Wiegand and Richardson, 1984; Sellers, 1985) but most rapidly for NDVI and TSAVI, and least rapidly for RVI and SAVI2 (Fig. 5). To exhibit this behavior, the relations must be curvilinear. However, considering the scatter in the data and the range in L , most authors chose to present linear equations. In Table 8, coefficients of determination, R^2 , are generally lower for the linear than for the nonlinear equations even for RVI and SAVI2, whose relations with L are least curvilinear. As stated earlier, the theoretical relation is nonlinear.

In part C of Table 8, FPAR(VI) relations from the literature are summarized. In principle, both FPAR and the vegetation indices are affected by solar zenith angle, canopy architecture, and soil background reflectance while the VI are additionally modestly affected by differences in wavelength intervals used and soil line slope. In reality, empirical fits are also affected by the distribution of the data points within the range of measurements and whether the full range of interest is contained in the data set. The NDVI equations included in Table 8 estimate FPAR to range from -0.37 to $+0.19$ for bare soil ($\text{NDVI} = 0.20$) and from 0.86 to 1.02 for a dense canopy ($\text{NDVI} = 0.90$). Among them the equation presented by Hatfield et al. (1984) is the best; it estimates $\text{FPAR} = 0$ at $\text{NDVI} = 0.155$ and $\text{FPAR} = 0.962$ at $\text{NDVI} = 0.95$, that is, for a very dense canopy. Its estimates parallel those of the equation of Baret et al. (1989). The equation of Hatfield et al. (1984) for estimating FPAR from pre- L_{\max} GVI also seems to be a good one since it estimates $\text{FPAR} = 0$ at $\text{GVI} = 0.5$ and $\text{FPAR} = 0.96$ at $\text{GVI} = 45$, that is, for GVI typical of bare soil and a canopy capable of absorbing nearly all the net downward PAR flux, $1 - R$, respectively. Neither the estimation of FPAR from SAVI2 nor the estimation of FPAR from the pooled PVI data from Weslaco and GVI data from Manhattan '83 (Fig. 7) can be recommended because we could not achieve a common relation between L and any of the VI, even through there was one for FPAR and L (Fig. 6).

In summary of Table 8 and the findings of this study (Table 4 and Figs. 5, 6, and 7), there is

general agreement, but the data presented herein argue for more nonlinear relations between L and VI and between FPAR and VI than indicated by Table 8. The fact that fits of $L(\text{VI})$ and $\text{FPAR}(L)$ for data pooled across locations were as good, and in some cases better than those for single experiments speaks well for the robustness of L and VI among experiments and for the ability to develop general relations to apply for wheat.

We thank all our technicians and colleagues who helped obtain and process the data. Special thanks go to Romeo Rodriguez for data analysis and figure preparation and to Saida Cardoza and Carol Harville for manuscript preparation.

REFERENCES

- Aase, J. K. (1978), Relationship between leaf area and dry matter in winter wheat, *Agron. J.* 70:563–565.
- Aase, J. K., and Tanaka, D. L. (1984), Effects of tillage practices on soil and wheat spectral reflectances, *Agron. J.* 76:814–818.
- Asrar, G., Fuchs, M., Kanemasu, E. T., and Hatfield, J. L. (1984), Estimating absorbed photosynthetically active radiation and leaf area index from spectral reflectance in wheat, *Agron. J.* 76:300–306.
- Baret, F., and Guyot, G. (1991), Potentials and limits of vegetation indices for LAI and APAR assessment, *Remote Sens. Environ.* 35:161–173.
- Baret, F., Guyot, G., and Major, D. J. (1989), TSAVI: A vegetation index which minimizes soil brightness effects on LAI and APAR estimation, in *Proc. IGARRS '90 / 12th Canadian Symp. on Remote Sens.*, Vancouver, Canada, 10–14 July 1989, vol. 3, pp. 1355–1358.
- Choudhury, B. J. (1987), Relationship between vegetation indices, radiation absorption, and net photosynthesis evaluated by sensitivity analysis, *Remote Sens. Environ.* 22: 209–233.
- Dusek, D. A., Jackson, R. D., and Musick, J. T. (1985), Winter wheat vegetation indices calculated from combinations of seven spectral bands, *Remote Sens. Environ.* 18:255–267.
- Garcia, R., Kanemasu, E. T., Blad, B. L., et al. (1988), Interception and use efficiency of light in winter wheat under different nitrogen regimes, *Remote Sens. Environ.* 44:175–186.
- Goel, N. S. (1988), Models of vegetation canopy reflectance and their use in estimation of biophysical parameters from reflectance data, *Remote Sens. Rev.* 4:1–212.
- Hatfield, J. L., Asrar, G., and Kanemasu, E. T. (1984), Intercepted photosynthetically active radiation estimated by spectral reflectance, *Remote Sens. Environ.* 14:65–75.
- Hatfield, J. L., Kanemasu, E. T., Asrar, G., et al. (1985), Leaf-area estimates from spectral measurements over various planting dates of wheat, *Int. J. Remote Sens.* 6:167–175.

- Hinzman, L. D., Bauer, M. E., and Daughtry, C. S. T. (1986), Effects of nitrogen fertilization on growth and reflectance characteristics of winter wheat, *Remote Sens. Environ.* 19: 47–61.
- Hipps, L. E., Asrar, G., and Kanemasu, E. T. (1983), Assessing the interception of photosynthetically active radiation in winter wheat, *Agric. Meteorol.* 28:253–259.
- Huete, A. R. (1989), Soil influences in remotely sensed vegetation-canopy spectra, in *Theory and Applications of Optical Remote Sensing* (G. Asrar, Ed.), Wiley, New York, pp. 107–141.
- Hughes, A. P., and Freeman, P. R. (1967), Growth analysis using frequent small harvests, *Appl. Ecol.* 4:553–560.
- Jackson, R. D. (1983) Spectral indices in *n*-space, *Remote Sens. Environ.* 13:409–421.
- Jackson, R. D., and Pinter, P. J., Jr. (1986), Spectral response of architecturally different wheat canopies, *Remote Sens. Environ.* 20:43–56.
- Jackson, R. D., Moran, M. S., Slater, P. N., and Biggar, S. F. (1987), Field calibration of reference reflectance panels, *Remote Sens. Environ.* 22:145–158.
- Kanemasu, E. T., Ranson, J., Saunders, D., Killeen, J., and Yosida, M. (1985), Use of spectral data to assess wheat response to soil water, *Field Crops Res.* 12:105–113.
- Lapitan, R. L. (1986), Spectral estimates of absorbed light and leaf area index: effects of canopy geometry and water stress, Ph.D. thesis, Department of Agronomy, Kansas State University, Manhattan.
- Large, E. G. (1954), Growth stages in cereals: illustration of the Feekes scale, *Plant Pathol.* 3:128–129.
- LeMaster, E. W., Chance, J. E., and Wiegand, C. L. (1980), A seasonal verification of the Suits spectral reflectance model for wheat, *Photogramm. Eng. Remote Sens.* 46:107–114.
- Maas, S. J., Jackson, R. D., Idso, S. B., Pinter, P. J., Jr., and Reginato, R. J. (1989), Incorporation of remotely-sensed indicators of water stress in a crop growth simulation model, in *Preprint Vol. 19th Conf. on Agric. and For. Meteorol.*, American Meteorology Society, Boston, pp. 228–231.
- Major, D. J., Blad, B. L., Bauer, A., et al. (1988), Winter wheat grain yield response to water and nitrogen on the North American Great Plains, *Agric. For. Meteorol.* 44: 141–150.
- Major, D. J., Baret, F., and Guyot, G. (1990), A ratio vegetation index adjusted for soil brightness, *Int. J. Remote Sens.* 11:727–740.
- Milliken, G. A., and DeBruin, R. L. (1978), A procedure to test hypotheses for nonlinear models, *Commun. Stat. Theor. Methods* A7(1):65–79.
- Pearson, R. L., and Miller, L. D. (1972), Remote mapping of standing crop biomass for estimation of productivity of the shortgrass prairie, Pawnee National Grasslands, Colorado, in *Proc. Eighth Int. Symp. on Remote Sens. Environ.*, vol. 2, Environ. Res. Inst. of Michigan, Ann Arbor, pp. 1355–1381.
- Pinter, P. J., Jr., Jackson, R. D., Ezra, C. E., and Gausman, H. W. (1985), Sun-angle and canopy-architecture effects on the spectral reflectance of six wheat cultivars, *Int. J. Remote Sens.* 6:1813–1825.
- Reginato, R. J., Hatfield, J. L., Bauer, A., et al. (1988), Winter wheat response to water and nitrogen in the North American Great Plains, *Remote Sens. Environ.* 44:105–116.
- Richardson, A. J. (1981), Measurement of reflectance factors under daily and intermittent irradiance variations, *Appl. Opt.* 20:3336–3340.
- Richardson, A. J., and Wiegand, C. L. (1977), Distinguishing vegetation from soil background information, *Photogramm. Eng. Remote Sens.* 43:1541–1552.
- Robinson, B. F., Bauer, M. E., DeWitt, D. P., Silva, L. F., and Vanderbilt, V. C. (1979), Multiband radiometer for field research, *Proc. Soc. Photo-Opt. Eng.* 196:8–15.
- Rouse, J. W., Jr., Haas, R. H., Schell, J. A., and Deering, D. W. (1974), Monitoring vegetation systems in the Great Plains with ERTS, in *Third ERTS Symp.*, NASA SP-351, U.S. Govt. Printing Office, Washington, DC, vol. I, pp. 309–317.
- SAS Institute Inc. (1988), *SAS / STAT™ User's Guide*, Release 6.03 Edition, SAS, Cary, NC.
- Sellers, P. J. (1985), Canopy reflectance, photosynthesis, and transpiration, *Int. J. Remote Sens.* 6:1335–1372.
- Sellers, P. J. (1987), Canopy reflectance, photosynthesis, and transpiration. II. The role of biophysics in the linearity of their dependence, *Remote Sens. Environ.* 21:143–183.
- Tucker, C. J., Jones, W. H., Kley, N. A., and Sundstrom, G. J. (1981), A three-band hand-held radiometer for field use, *Science* 211:281–283.
- Verhoef, W. (1984), Light scattering by leaf layers with application to canopy reflectance modeling: The SAIL model, *Remote Sens. Environ.* 16:125–141.
- Wall, G. W., and Kanemasu, E. T. (1990), CO₂ exchange rates in wheat canopies. II. Photosynthetic and phytomass efficiencies, *Agric. For. Meteorol.* 49:103–122.
- Walter-Shea, E. A., and Biehl, L. L. (1990), Measuring vegetation spectral properties, *Remote Sens. Rev.* 5:179–205.
- Wiegand, C. L., and Hatfield, J. L. (1988), The spectral-agronomic multisite-multicrop analyses (SAMMA) project, *Int. Arch. Photogramm. Remote Sens.* 27(B7):696–706.
- Wiegand, C. L., and Richardson, A. J. (1984), Leaf area, light interception, and yield estimates from spectral components analysis, *Agron. J.* 76:543–548.
- Wiegand, C. L., and Richardson, A. J. (1987), Spectral components analysis: rationale and results for three crops, *Int. J. Remote Sens.* 8:1011–1032.

- Wiegand, C. L., and Richardson, A. J. (1990), Use of spectral vegetation indices to infer leaf area, evapotranspiration and yield: II. Results, *Agron. J.* 82:630–636.
- Wiegand, C. L., Gerbermann, A. H., Gallo, K. P., Blad, B. L., and Dusek, D. (1990), Multisite analyses of spectral-biophysical data for corn, *Remote Sens. Environ.* 33: 1–16.
- Wiegand, C. L., Shibayama, M., Yamagata, Y., and Akiyama, T. (1989) Spectral observations for estimating the growth and yield of rice, *Jpn. J. Crop Sci.* 58:673–683.